مراقبة الجهد من المولد ذاتي الانفعال (SEIG) باستخدام المولد مزدوج التغذية (DFIG) ومعوض التوزيع الثابت (D-STATCOM) دراسة مقارنة

كاليان راج كانيغانتي وسرينفاسا راو رايابودي

* قسم الهندسة الكهربائية، جواهر لال نهرو الجامعة التكنولوجية، الهند

الخــلاصـة

أدت التطورات في الأجهزة الإلكترونية للطاقة إلى زيادة القدرة على التحكم في تدفق الطاقة التفاعلي في الشبكة. ويتحقق ذلك باستخدام أجهزة الحقائق مع استراتيجيات التحكم المتقدمة. في السنوات الأخيرة يتم استغلال قدرات القدرة على رد الفعل من (DFIG) أيضا. (SEIG) هو مولد رياح معروف التكوين يستخدم في كل من الشبكة المعزولة والشبكة المتصلة. تواجه (SEIG) مشكلة عدم استقرار الجهد خلال سرعة الرياح المتفاوتة وظروف الاحمال، مما يؤدي الى تأثير سلبي على الشبكة المتصلة. ويمكن أن تساعد متطلبات القدرة التفاعلية التي يوفرها مصدر خارجي المولد على العمل في منطقة مستقرة. في هذه الورقة يتم تحليل مفصل لدراسة تفوق (DFIG)على (D-STATCOM) في السيطرة على الجهد الناتج من (SEIG). لهذا، يتم اشتقاق نموذج السعة المكافئ الجديد من (DFIG) لشرح قدرات التعامل مع القدرة التفاعلية من (DFIG). ويستخدم مؤشران: متوسط الجهد ومعدل العقد منخفضة الجهد (RUVMN) لمقارنة المزايا التشغيلية لكلا الأسلوبين. ويتم التحليل لسرعات الرياح المختلفة والنتائج تبين أن التحكم في الجهد مع (DFIG)هو أفضل بالمقارنة مع (D-STATCOM).

Voltage control of SEIG using D-STATCOM and DFIG: a comparative study

Kalyan Raj Kaniganti* and Srinivasa Rao Rayapudi**

Department of Electrical Engineering, Jawaharlal Nehru Technological University, India

Corresponding Author: kalyan20.kaniganti@gmail.com

ABSTRACT

The advancements in power electronic devices have increased the ability of controlling the reactive power flow in the network. This is achieved by using facts devices with advanced control strategies. In recent years, reactive power supplying capabilities of DFIG is also exploited. SEIG is a well-known wind generator configuration used in both isolated and grid connected modes. SEIG experiences a problem of voltage instability during varying wind speeds and load conditions, which shows a negative impact on the connected network. The reactive power requirement supplied by an external source can assist the generator in operating in stable regions. In this paper, a detailed analysis is done to examine the superiority of DFIG over D-STATCOM in voltage control of SEIG. For this, a novel equivalent capacitance model of DFIG is derived to explain reactive power handling capabilities of DFIG. Two indices, average voltage profile and RUVMN, are used to compare the operational advantages of both techniques. The analysis is done with varying wind speeds, and results show that voltage control with DFIG is better when compared to D-STATCOM.

Keywords: Capacitance; Distribution Static Compensator (D-STATCOM); doubly fed induction generator (DFIG); reactive power requirement; self-excited induction generator (SEIG); stabilization.

Abbreviations

Symbol	Abbreviation	Symbol	Abbreviation
P_{mech}	Mechanical power output	X_m	Magnetizing reactance
R_s	Stator resistance	X_c	Capacitive reactance
R_r	Rotor resistance	I_s	Stator current
R_l	Load resistance	I_r	Rotor current
L_s	Stator inductance	f	Frequency
L_r	Rotor inductance	s	Slip
L_m	Mutual inductance	P_e	3-ϕ Active power output
S	Total power	Q_e	3-ϕ Reactive power output

INTRODUCTION

In recent years, wind turbines driven by induction generators are widely used because of their adaptive nature in varying torque and speed conditions. Among the available technologies, SEIG is the most simple in construction and self-protecting nature during short circuit conditions (Bansal, 2005). SEIG faces the problem of voltage inastability because terminal voltage build-up depends on the value of excitation capacitance and load mix for particular generator speed (Mustafa *et al.*, 1988; Malik *et al.*, 1987). In case of low generator speeds or high loading conditions, if no external reactive power source is used, SEIG acts as an additional reactive load on the network, which may lead to system collapse. In order to pull the generator into stable region, the reactive power required for self-excitation should be supplied by an external source. The value of the generated voltage, irrespective of its frequency, can be controlled using variable capacitance values (Kheldoun *et al.*, 2012). This method is limited due to lack of continuous control. Rajambal explained a method of using breaking resistors for improvement of SEIG stability, but this method is of slow response. An advanced logical pitch control method is discussed in Muyeen *et al.* (2006), which can control only active power flow and not reactive power. Muyeen *et al.* (2006) and Saoud *et al.* (1998) discussed the ability of D-STATCOM in controlling reactive power flow in wind farms. The advancements in facts devices made the control of reactive power smooth and wide, and their application in distribution load flow is presented in Hosseini *et al.* (2008). Different methods proposed for voltage control of SEIG are summarized in Hasan Ali *et al.* (2010). Only few attempts (Hasan Ali *et al.*, 2007; Divya *et al.*, 2006) were made to analyse the effect of scenarios like underexcitation and reactive power handling capabilities of wind generators on the distribution system. Particularly, DFIG has additional capability of providing reactive power support to the network even at low wind speeds, which is possible by magnetization supplied by the rotor side converter (Ullahand *et al.*, 2007). This method of reactive power control enhances stability of the network without additional equipment, thereby reducing the cost. Many authors proposed different techniques of reactive power control capabilities of DFIG (Kayikci *et al.*, 2007; Ekanayake *et al.*, 2003; Tapia *et al.*, 2003; Feijóo *et al.*, 2010; Dadhani *et al.*, 2013; Takahashi *et al.*, 2006; Chowdhury *et al.*, 2006; Mohseni *et al.*, 2011; Lie Xu *et al.*, 2006; Foster *et al.*, 2010; Dao. *et al.*, 2015). At the point when voltage control necessity is beyond the ability of a SEIG, the voltage stability of a grid will be influenced. A DFIG or a reactive power source like D-STATCOM installed on the network having SEIG can supply reactive power requirement of SEIG, retaining its generating capability and also increasing system stability. The effect of D-STATCOM on the stability of network having SEIG has been addressed in numerous works. Only little literature was available on studying the effect of DFIG in its reactive power control mode on the distribution system. In this paper, an attempt is made to study the effect of underexcited SEIG on the network and the ability of D-STATCOM and DFIG to stabilize SEIG. For this, a new methodology of representing DFIG, in terms of its equivalent capacitance independent of D-Q theory, is proposed to study reactive power handling capabilities of DFIG and its ability to stabilize SEIG, thereby improving the network stability. The analysis is done on standard IEEE 33-bus system.

The rest of the paper is organized as follows. Minimum capacitance requirement and power flow model of SEIG are presented in the next section. Results pertaining to voltage control of SEIG with D-STATCOM and proposed equivalent capacitance model of DFIG are discussed next. The analysis of results follows next. Conclusions are presented in the last section.

MODELING AND ANALYSIS OF WIND TURBINE

Modeling of wind turbine

The wind turbine generating unit is comprised of wind turbine and Induction Generator unit. Wind turbine converts kinetic energy in the wind into mechanical power required for the generator. The wind power is given by

$$P_w = \frac{dW_w}{dt} \tag{1}$$

The energy drawn by the wind turbine is

$$W_w = \frac{1}{2}\rho\left(V_1^2 - V_2^2\right) \tag{2}$$

where ρ=air density, V1 = velocity of wind, and V2 =wind velocity at the turbine rotor.

The wind power is given as
$$P_w = \frac{d\left[V_a \frac{1}{2}\rho\left(V_1^2 - V_2^2\right)\right]}{dt} \tag{3}$$

According to the Betz maximum power output of the turbine,

$$P_w = \frac{16}{27}\frac{\rho}{2}V_1^3 A_R \tag{4}$$

where AR is area swept by rotor.

The mechanical power developed by the turbine is

$$P_m = \frac{1}{2}\rho V_w^3 . C_p \tag{5}$$

where $C_p = C_1(\frac{1}{\kappa}C_2 C_3 \upsilon - C_4 v^3 - C_5)e^{\frac{-C_6}{k}}$ and $\frac{1}{\kappa} = \frac{1}{(\lambda + 0.08v)} - \frac{0.035}{(1+v^3)}$

The lambda value is obtained from the power coefficient curve $C_p(\lambda,v)$ and Vw is the wind velocity. The theoretical maximum power extractable from wind is 16/27 times the power contained in the wind. For most of wind turbines, operating speed is normally between 8 and 16m/s.
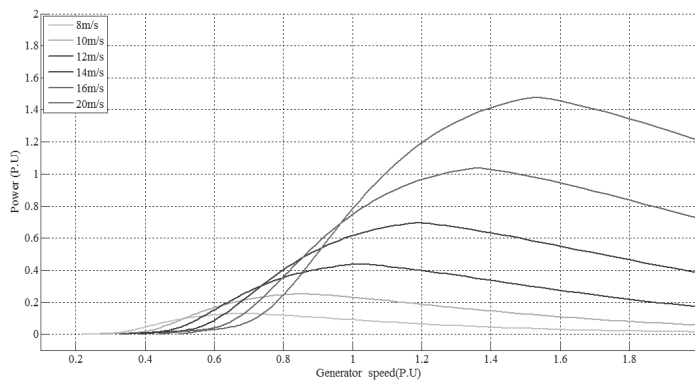

Figure 1. Wind turbine characteristics.

The characteristics of wind turbine (1.5MW) are obtained for different wind speeds as shown in Figure 1. From the figure, it is seen that the maximum power obtained is 73% at rated wind speed of 14m/s and generator speed of 1.2 (p.u). The P_{mech} output of a wind turbine for a given wind speed is shown in Table 1.

Table 1. Mechanical power output of turbine at different wind speeds.

Wind speed (m/s)	P_{mech} (MW)	Power (p.u)
8	-0.22	0.153
10	-0.37	0.25
12	-0.66	0.44
14	-1.09	0.73
16	-1.57	1.04

From Table 1, it is seen that as wind speed increases, the power generated by the turbine increases. The negative sign in Table 1 indicates that the power is generated by the turbine. This value of output power of wind turbine is embedded as mechanical input to the induction generator models.

Modeling and analysis of SEIG

When a capacitor bank is connected at stator terminals of an induction machine driven by a wind turbine, it acts as an induction generator. The terminal voltage build-up of SEIG depends on capacitance and load mix for a particular generator speed. In this paper, the load is supposed to be kept constant, and the minimum capacitance requirement for different generator speeds is given in Table 2 (Malik *et al.*, 1987). The method of calculating equivalent capacitance is explained in the appendix.

Table 2. Capacitance requirement of SEIG for different generator speeds.

Wind speed (m/s)	Generator speed (rads/sec)	Minimum capacitance(μF)
12	157.5	68
10	133	83
9.5	125	90
9	117	98
8	102	106

From the results, it is observed that the capacitance value required for the generator to self-excite decreases as the generator speed increases. SEIG generates power at rated voltage until reactive power requirement of generator is satisfied or else, the generator falls into underexcited region and fails to build voltage. The corresponding active and reactive power outputs of the generator are calculated using Equation (6) and Equation (7), respectively.

$$P_e = \frac{sR_rV^2}{R_r^2 + s^2(X_s + X_r)^2} \tag{6}$$

$$Q_e = \frac{A}{B} \tag{7}$$

where A is expressed as

$$[X_mX_rs^2(X_m + X_r) + X_ss^2(X_m + X_r)^2 + R_s^2(X_m + X_s)]V^2$$

and B is expressed as

$$[R_sR_r + s(X_m^2 - (X_m + X_r)(X_m + X_s))]^2 + [R_r(X_m + X_s) + sR_s(X_m + X_r)]^2$$

In practical case capacitance across the generator is kept constant at the value required during the base wind speed. When wind speed reduces below base value SEIG falls into undervoltage region as shown in Table 3.

Table 3. Voltage build-up at different wind speeds.

Wind speed (m/s)	Speed (p.u)	(V_t) kV (per phase)	Excitation capacitance (p.u)	P_e MW	Q_e MVAr
12	0.9	1.36	1.0	0.65	0.023
10	0.85	1.00	1.0	0.27	0.003
9.5	0.8	Voltage collapse	1.0	--	--
9	0.75	Voltage collapse	1.0	--	--
8	0.7	Voltage collapse	1.0	--	--

From the results, it is observed that when wind speed is reduced below 10m/s, the terminal voltage of SEIG collapses and tries to draw reactive power from the network. This has negative impact on the network and is explained below. In the entire analysis, wind speed is considered between 12 and 8m/s because SEIG starts to fall into underexcitation in this range of wind speed. So, the comparison of methods at base wind speed (14m/s) is not discussed in this paper.

SIMULATION RESULTS

Voltage control of SEIG can be achieved by supplying the necessary reactive power to drive the machine into saturation region. In this paper, two methods for voltage control of SEIG are presented. The first method is supplying the necessary reactive power from D-STATCOM (case 1). The second is a proposed novel method done by varying the excitation capacitance virtually, utilizing the reactive power handling capabilities of DFIG (case 2). DFIG, in terms of its equivalent capacitance, is modeled, and the interaction of DFIG during this mode with SEIG is analysed in this section. For comparison of discussed methods, two indexes are proposed in this paper.

The average voltage profile is given by

$$AV = \frac{sum(V_{bus})}{n_{total}} \tag{8}$$

The other index is the rate of undervoltage mitigated nodes (RUVMN) and is given by

$$\%RUVMN = \frac{n_p - n_{total}}{n_{base}} * 100 \tag{9}$$

where ntotal is total number of buses; nbase is the number of buses facing undervoltage problem in base case; np is number of buses not facing undervoltage problem. % RUVMN depicts the number of buses facing undervoltage problem, as the value increases the number of under voltage buses increases, reducing system stability and vice versa. Average voltage profile also resembles system stability, and the increase in average voltage indicates good system stability.

Case 1: voltage control of SEIG with STATCOM

D-STATCOM is a suitable device among FACTS for stabilization of SEIG when smooth control and cost effectiveness are considered. In this section, D-STATCOM model for distribution load flow proposed in M. Hosseini *et al.* (2008) is considered for analysis. The reactive power requirement of SEIG during varying wind speeds is supplied by the D-STATCOM, when both are connected adjacent to each other as shown in Figure 2(a). SEIG and D-STATCOM are connected at same bus and the analysis is done for different wind speeds (12-8m/s). DFIG of 1.5 MW and D-STATCOM of 1MVA are considered in this analysis because of their equivalence in terms of reactive power supplying capability. The difference is that DFIG supplies additional active power along with reactive power support, whereas STATCOM can provide only reactive power support. The power flow during different wind speeds is given in Figure 2(a). Figure 2(b) gives the capability curve of STATCOM connected wind plant. From the figure, it is observed that the reactive power capacity of STATCOM is limited to 0.3 p.u in dynamic capability range and 0.446 p.u in continuous control range for maximum power generation of 1 p.u.
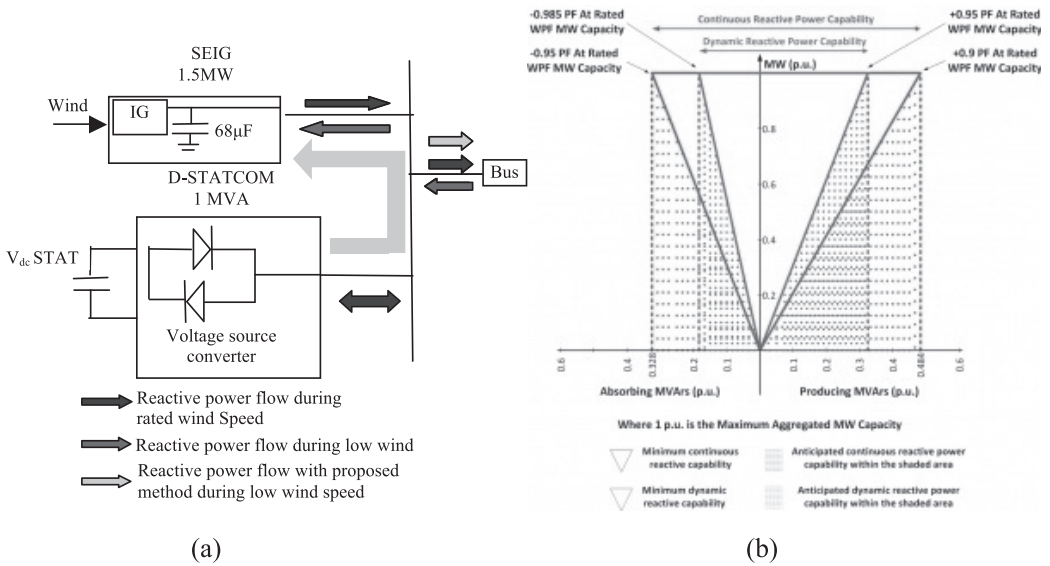

(a)   (b)

Figure 2. (a) Power flow during different wind speeds for

case 1; (b) capability curve of D-STATCOM based wind plant.

During low power generation, that is, at 0.2 p.u, also the dynamic range is 0.05 - 0.3 p.u and continuous control capability is 0.1-0.446 p.u. In the case of DFIG, the range is a bit more and is explained in the following section.

The ability of D-STATCOM to maintain network stability as well as voltage control of SEIG is shown in terms of power loss, RUVMN, and average voltage in Figures 3 to 6.
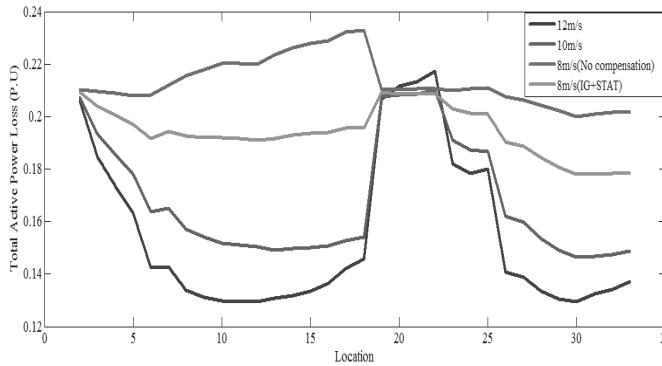
Figure 3. Total active power loss at different locations for case 1.

The results from Figure 3 show that power loss varies with variation in wind speed. At wind speed of 12 m/s, power loss reduces to 0.1294 p.u., less than base case (given in the appendix, Table A2).When wind speed reduces to 8m/s ,the scenario changes and power loss reaches to 0.2011 p.u., almost equal to base case and it is more than base case in some locations (7 to 25).
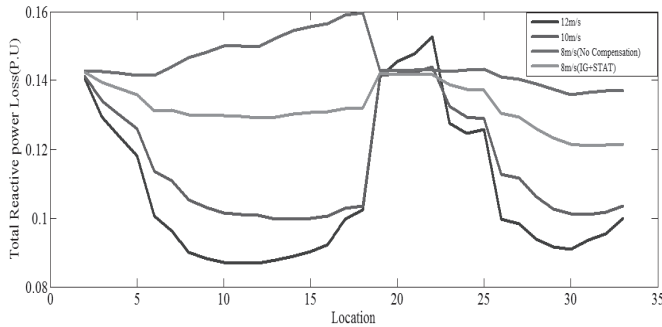

Figure 4. Total reactive power loss at different locations for case 1.

In case of reactive power loss shown in Figure 4, reactive power loss is low in major locations at wind speed of 12 m/s. When wind speed reduces to 8 m/s, the reactive power loss in all the locations is more than base case as SEIG tries to draw reactive power from utility.
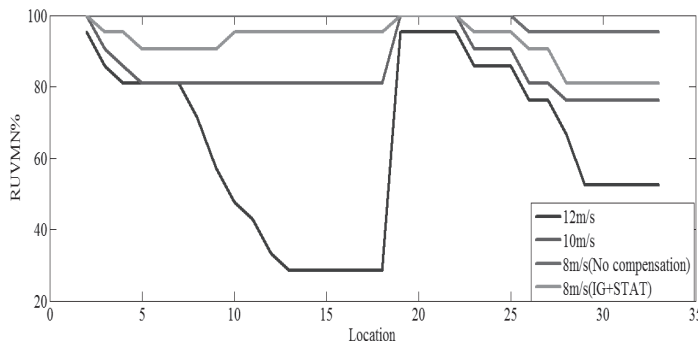
Figure 5. % RUVMN at different locations for case 1.

From Figure 5, it is seen that the value of RUVMN at 12 m/s wind speed is 28% and it reaches 0% when the generator is operated at base speed of 14m/s. SEIG will not draw reactive power from the grid and it generated rated active power at base wind speed of 14 m/s. At low wind speed of 8 m/s, 100% of buses are facing undervoltage problem in almost all the locations, threatening the system stability.
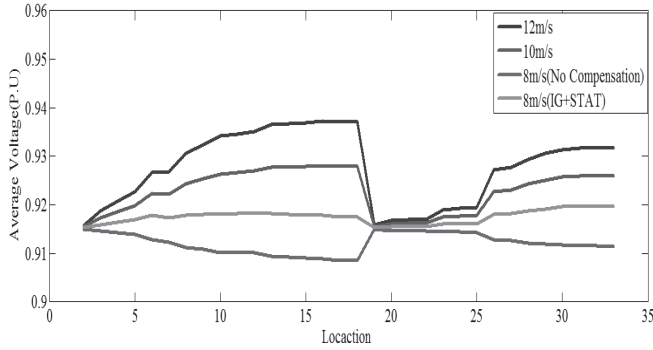
Figure 6. Average voltage profile at different locations for case 1.

From Figure 6, it is seen that, at low wind speed of 8m/s, the average voltage profile is less than the base case value. It is also observed that the average voltage profile increases with the increase in wind speed.

Table 4. Performance of D-STATCOM at different wind speeds.

SEIG+ D-STATCOM	Ploss (p.u)		Qloss (p.u)		Average voltage (p.u)		% RUVMN	
Location	12m/s	8m/s	12m/s	8m/s	12m/s	8m/s	12m/s	8m/s
2	0.2059	0.2103	0.1405	0.1428	0.9158	0.9150	95.2381	100
3	0.1845	0.2097	0.1293	0.1425	0.9188	0.9146	85.7143	100
4	0.1738	0.2089	0.1237	0.1421	0.9208	0.9143	80.9524	100
5	0.1632	0.2078	0.1181	0.1415	0.9228	0.9140	80.9524	100
6	0.1426	0.2082	0.1005	0.1415	0.9267	0.9129	80.9524	100
7	0.1427	0.2119	0.0964	0.144	0.9268	0.9123	80.9524	100
8	0.1337	0.2155	0.0899	0.1466	0.9306	0.9113	71.4286	100
9	0.1313	0.2178	0.0881	0.1483	0.9325	0.9108	57.1429	100
10	0.1298	0.2202	0.087	0.15	0.9342	0.9102	47.619	100
11	0.1296	0.2201	0.0869	0.1499	0.9345	0.9102	42.8571	100
12	0.1294	0.22	0.0868	0.1497	0.9351	0.9101	33.3333	100
13	0.1307	0.2235	0.0877	0.1523	0.9365	0.9095	28.5714	100
14	0.1317	0.2263	0.0888	0.1545	0.9367	0.9092	28.5714	100
15	0.1336	0.2278	0.0903	0.1557	0.9369	0.9091	28.5714	100
16	0.1364	0.2289	0.0923	0.1565	0.9372	0.9089	28.5714	100
17	0.1422	0.2321	0.0996	0.1591	0.9371	0.9086	28.5714	100
18	0.1459	0.2327	0.1024	0.1596	0.9371	0.9085	28.5714	100
19	0.2065	0.2103	0.141	0.1428	0.9159	0.9150	95.2381	100
20	0.2116	0.2104	0.1456	0.1429	0.9168	0.9147	95.2381	100
21	0.2133	0.2105	0.1477	0.143	0.9169	0.9147	95.2381	100
22	0.2172	0.2106	0.1528	0.143	0.917	0.9146	95.2381	100
23	0.182	0.2098	0.1276	0.1426	0.919	0.9145	85.7143	100
24	0.1784	0.2105	0.1247	0.143	0.9194	0.9144	85.7143	100
25	0.1799	0.211	0.1258	0.1433	0.9195	0.9143	85.7143	100
26	0.1409	0.2075	0.0996	0.1411	0.9272	0.9128	76.1905	95.2381
27	0.1388	0.2064	0.0984	0.1404	0.9278	0.9127	76.1905	95.2381
28	0.1334	0.2043	0.0939	0.1389	0.9294	0.9122	66.6667	95.2381
29	0.1304	0.2023	0.0915	0.1375	0.9306	0.9119	52.381	95.2381
30	0.1294	0.1998	0.0909	0.1359	0.9313	0.9118	52.381	95.2381
31	0.1324	0.2011	0.0936	0.1366	0.9317	0.9115	52.381	95.2381
32	0.134	0.2016	0.0954	0.1369	0.9317	0.9115	52.381	95.2381
33	0.1371	0.2017	0.0998	0.137	0.9317	0.9114	52.381	95.2381

From the results in Table 4, it is observed that, for wind speed of 12 m/s, the number of buses facing undervoltage problem is 28% when the location was 13 to 17 buses and the maximum average voltage was 0.9372 p.u at location 16. The minimum active power loss is 0.1294 p.u and reactive power loss is 0.0868 p.u at location 12. When wind speed reduces to 8m/s, the point at which SEIG loses its self-excitation, the effect on connected network is high. The minimum RUVMN is 95% from location 26 to 33 and the rest of the locations suffer from 100% undervoltage nodes. The maximum average voltage falls to 0.9080 p.u; active and reactive power loss increase to 0.1998 p.u and 0.1359 p.u, respectively. At the instant when STATCOM is supplying necessary reactive power to SEIG, it generates power at rated voltage. The active and reactive power loss reduce to 0.1779 p.u and 0.1654 p.u, respectively as shown in Figure 4. From Figure 5 it is observed that only 3 locations have 100% undervoltage nodes and RUVMN decreases by 5%, that is, 80.95. The maximum average voltage increases to 0.9196 p.u as shown in Figure 6. The results show that, with injection of reactive power from the STATCOM, SEIG is able to generate power at rated voltage, thereby increasing overall system stability.

Case 2: voltage control of SEIG with DFIG

DFIG connected adjacent to SEIG can supply reactive power requirements during low wind speeds and this methodology is explained in detail in this section. In DFIG due to presence of back to back converters, it is capable of controlling reactive power output (Dao. Z *et al.*, 2015). The steady state model of DFIG is explained in detail in Feijóo *et al.* (2010). From the literature, proportionality of reactive power output with rotor side converter current limit is observed. Using the capability of power electronic switches to withstand currents of 150 % of rated value, reference of rotor side converter current is changed depending on reactive power requirement. The reactive power output depends on the rotor side converter rating, which is usually 30% and, in an exceptional case, 50% of the generator rating. In this work, the analysis is done for 30% rotor converter rating. The steady state equations for deriving the characteristics of DFIG are given by

Equations (10-12)

$$V_s \angle \psi_s = R_s + j(X_s + X_m))I_s \angle \phi_s + jX_m I_r \angle \phi_r \qquad (10)$$

$$V_r \angle \psi_r = R_r + j(X_r + X_m))I_r \angle \phi_r - jX_m I_s \angle \phi_s \qquad (11)$$

The relation between stator and rotor voltages is given as

$$V_r = jX_r I_r + \frac{X_m}{X_s} s V_s \qquad (12)$$

Substituting (12) in (11), we can obtain two equations having two unknown variables. There are two equations having two unknowns which are solved using Newton-Raphson iterative method. Solving these equations gives the value of Is and Ir, that is, the stator and rotor currents.   From the literature, it is observed that the reactive power of DFIG depends on rotor side converter current limit.   To represent this analytically, a new term 'K' as given in Equation (19) is introduced into DFIG steady state equations. This term resembles the reference current limit of rotor side converter and it varied between 1 and 1.5. The values of rotor side current and stator side current during reactive power control mode are calculated by solving the modified equations obtained by substituting Equation (19) in Equations (10-12). By using Equation (21), the reactive power can be

converted into equivalent capacitance. The algorithm for deriving equivalent capacitance of DFIG is explained in Figure 7.

The real and reactive power outputs of the grid side VSC reaching a point of common coupling (PCC), when DC link is considered lossless [20], are given by

$$P_r = real\left\{ V_s \left[\frac{V_s - V_r}{Z_g} \right]^* \right\} \tag{13}$$

$$Q_r = imag\left\{ V_s \left[\frac{V_s - V_r}{Z_g} \right]^* \right\} \tag{14}$$

where Z_g is the combined impedance of grid side and rotor side converter and its value is given in the appendix.
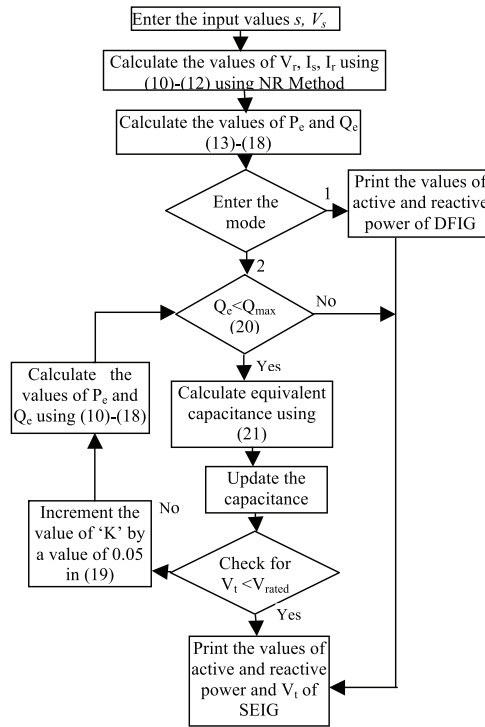

Figure 7. Flow chart for the proposed model.

The real and reactive powers of the wound rotor induction machine are given from the following equations:

$$P_s = real[V_s I_s^*] \tag{15}$$

$$Q_s = imag[V_s I_s^*] \tag{16}$$

Total active power: $P_e = P_s + P_r \tag{17}$

Total Reactive power: $Q_e = Q_s + Q_r \tag{18}$

$$I_{rnew} = I_r * K \tag{19}$$

$$Q_{\max} = \sqrt{S^2 - P_r^2} \tag{20}$$

$$X_c = \frac{Q_e}{I_s^2 \sin(\tan^{-1} \frac{Q_e}{P_e})} \tag{21}$$

The value of X_c in Equation (21) gives equivalent capacitive reactance value of DFIG. The value of 'K' varied until the equivalent capacitance value obtained matches the required capacitance value required by SEIG to self-excite. Mode 1 in the flow chart indicates normal operation of DFIG and mode 2 indicated reactive power control mode of DFIG. The program converges when equivalent capacitance value reaches desired capacitance value for SEIG to self-excite, provided the value of 'K' is less than 1.5 and X_c is equal to the value obtained from Table 2.

The equivalent capacitance of DFIG at different wind speeds is given in Table 5. From the table, it is seen that, by increasing the current limit of rotor side converter, reactive power produced by DFIG increases and hence enhances its capabilities. As wind speed reduces rotor side converter is made to draw current from utility and injects more reactive currents to the stator side, and thus the equivalent capacitance value increases. The developed model demonstrates reactive power handling capabilities of DFIG very well. The value of equivalent capacitance obtained is added across SEIG. SEIG starts to generate power at rated voltage as given in Table 5.

Table 5. Equivalent capacitance of DFIG at different wind speeds.

Wind speed (m/s)	Rotor converter current	Equivalent capacitance (µF)	Capacitance (p.u)	Total excitation capacitance (p.u)	V_t kV	P_e MW
12	$I_{rnew}=I_r$	10.2	0.15	1.0	1.36	0.65
10	$I_{rnew}=I_r$	15.5	0.23	1.0+0.23	1.36	0.39
9.5	$I_{rnew}=1.24I_r$	22.56	0.32	1.0+0.32	1.36	0.31
9	$I_{rnew}=1.45I_r$	30.3	0.43	1.0+0.43	1.36	0.263
8	$I_{rnew}=1.48I_r$	37.4	0.55	1.0+0.55	1.36	0.22

The robustness of the model is also tested during variable load conditions. The analysis is done for possible low wind speed of 8m/s and the load varied from 0.5 to 1.0 p.u. The low wind speed (8m/s) and high load (1.0 p.u) are the worst possible case the generator experiences; hence, the effectiveness of the proposed model can be well validated. The results in Table 6 show that for low wind speed reactive power requirement of SEIG increases with load. During this case DFIG changes its mode as reactive power source and supplies the necessary reactive power for SEIG to retain the generating capabilities.

Table 6. Equivalent capacitance of DFIG for different loads at low wind speed.

Speed (rad/s)	Load on SEIG (p.u)	Voltage build-up without DFIG (kV)	Capacitance added from DFIG (p.u)	Capacitance required by SEIG (p.u)	Rotor side converter current of DFIG	Equivalent capacitance added per phase (µF)	V_t (kV)
102	0.5	1.36	Nil	0.64	$I_{rnew}=I_r$	Nil	1.36
	0.6	1.36	Nil	0.86	$I_{rnew}=I_r$	Nil	1.36
	0.7	--	0.10	1.0+0.10	$I_{rnew}=1.12I_r$	7	1.36
	0.8	--	0.32	1.0+0.38	$I_{rnew}=1.32I_r$	26	1.36
	0.9	--	0.51	1.0+0.51	$I_{rnew}=1.40Ir$	34.5	1.36
	1.0	--	0.55	1.0+0.55	$I_{rnew}=1.48I_r$	37.4	1.36

From the above table, it is observed that at low generator speed of 102 rad/s and load of 1.0 p.u DFIG supplies an equivalent capacitance of 37.4 μF per phase at a 'K' value of 1.45. The reactive power exchange between SEIG, DFIG, and network at different wind speeds is depicted clearly in Figure 8(a). Figure 8(b) gives the reactive power capacity of DFIG connected wind plant. During full rated power generation (1p.u) and slip of -0.2, the reactive power capability ranges from 0.3 to 0.4 p.u. During low speed operation or subsynchronous generation mode at power generation of 0.2 p.u, the reactive power capability ranges from 0.05 to 0.8p.u, which is not possible in the case of D-STATCOM.
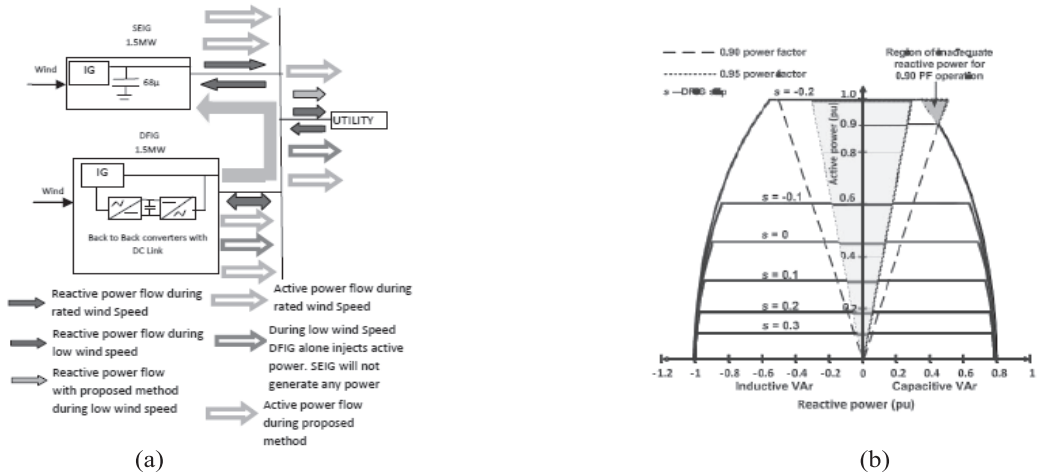

Figure 8. (a) Power flow at different wind speeds for case 2;
(b) DFIG reactive power capability curve [Foster *et al.*, 2010].

Since the work in papers is to enhance the generating capability of SEIG at low wind speed, the comparison of capability curves of DFIG and D-STATCOM proves the superiority of proposed method both in active and reactive power support to the network connected.

Active power losses at different locations during different wind speeds in case 2 are shown in Figure 9. The variation of reactive power loss at different wind speeds is observed in Figure 10. The average voltage and RUVMN at different locations for the proposed method are shown in Figure 11 and Figure 12, respectively.
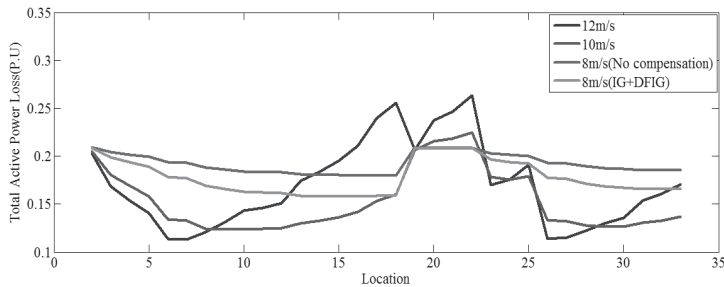

Figure 9. Total active power loss at different locations for case 2.

The results in Figure 9 show that, at wind speed of 12m/s, active power loss at location 7 reduced to 50 % of that during the base case .But in some locations (17 to 22), the total loss is more

than that of the base case. Since both DFIG and SEIG are injecting active power, these locations (17 to 22) are not considered as optimal locations. During low wind speed of 8 m/s also the power loss is less than that of the base case in the majority of locations.
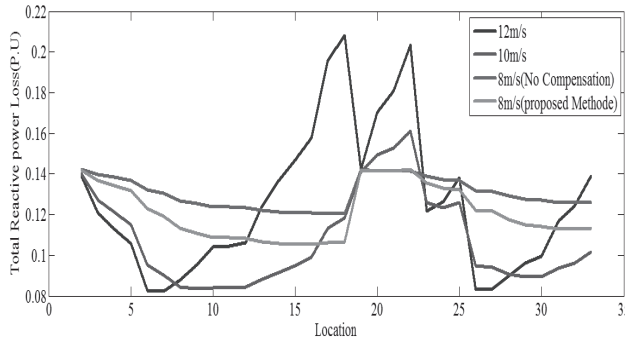

Figure 10. Total reactive power loss at different locations for case 2.

From Figure 10 it seen that as wind speed increases reactive power loss in the network decreases. At low wind speed (8m/s) the power loss is less than that of the base case in the majority of locations because DFIG is injecting active power even though SEIG is acting as a reactive load.
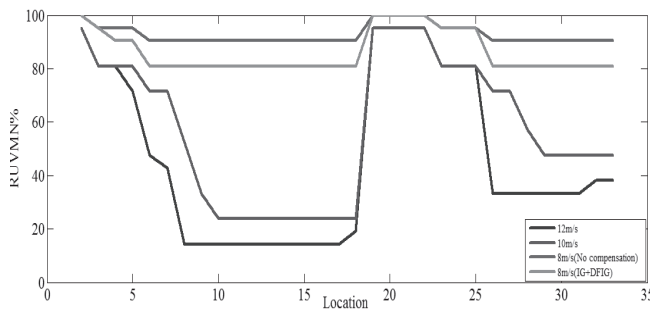
Figure 11. % RUVMN at different locations for case 2.

At wind speed of 12 m/s only 14% of the buses are facing undervoltage problem as shown in Figure 11 and this reaches to 0% when wind speed increases to 14 m/s. Since both generators produce rated power at 14 m/s, no bus in the network faces undervoltage problem. The point of interest in the paper is the generator behavior at low wind speeds. The results at rated wind speed are not depicted in the paper. At low wind speed (8m/s) 90% of the buses face undervoltage problem in the majority of locations, which is less compared to case 1.

Figure 12. Average voltage profile at different locations for case 2.

At wind speed of 14m/s the system experiences a good acceptable average voltage profile because both SEIG and DFIG are supplying active power. At low wind speed (8m/s) during uncompensated scenario the majority of locations have average voltage value less than that of the base value.
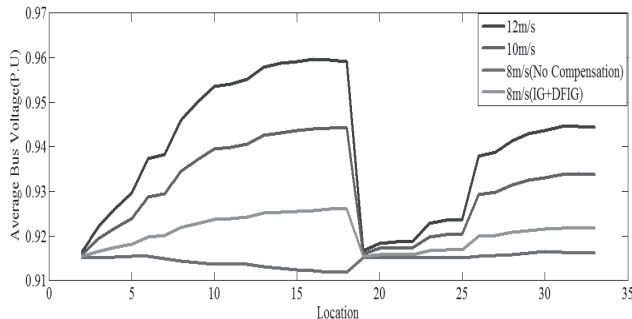
Table 7. Performance of DFIG at different wind speeds.

SEIG+ DFIG	Ploss (p.u)		Qloss (p.u)		Average voltage (p.u)		% RUVMN	
Location	12m/s	8m/s	12m/s	8m/s	12m/s	8m/s	12m/s	8m/s
2	0.2029	0.2093	0.1389	0.1423	0.9164	0.9151	95.2381	100
3	0.1685	0.2043	0.1209	0.1397	0.9222	0.9152	80.9524	95.2381
4	0.154	0.2017	0.1131	0.1383	0.926	0.9153	80.9524	95.2381
5	0.1404	0.1991	0.1058	0.137	0.9297	0.9154	71.4286	95.2381
6	0.1134	0.1935	0.0829	0.1323	0.9374	0.9154	47.619	90.4762
7	0.1131	0.1928	0.0822	0.1303	0.9383	0.9149	42.8571	90.4762
8	0.1208	0.188	0.0877	0.1268	0.9461	0.9144	14.2857	90.4762
9	0.1315	0.1858	0.0953	0.1253	0.9501	0.914	14.2857	90.4762
10	0.1434	0.1839	0.1039	0.1239	0.9535	0.9136	14.2857	90.4762
11	0.1459	0.1835	0.1047	0.1237	0.9541	0.9136	14.2857	90.4762
12	0.1512	0.183	0.1063	0.1235	0.9551	0.9137	14.2857	90.4762
13	0.1742	0.1811	0.1243	0.122	0.9579	0.9131	14.2857	90.4762
14	0.1837	0.1805	0.1367	0.1213	0.9587	0.9127	14.2857	90.4762
15	0.1953	0.1801	0.1469	0.121	0.9592	0.9125	14.2857	90.4762
16	0.2105	0.1798	0.1578	0.1208	0.9596	0.9123	14.2857	90.4762
17	0.2394	0.1796	0.1959	0.1205	0.9595	0.9119	14.2857	90.4762
18	0.2555	0.1797	0.2081	0.1206	0.9592	0.9118	19.0476	90.4762
19	0.2063	0.2092	0.1422	0.1422	0.9167	0.9151	95.2381	100
20	0.2374	0.2085	0.1702	0.1416	0.9184	0.9151	95.2381	100
21	0.2465	0.2084	0.1808	0.1415	0.9187	0.9151	95.2381	100
22	0.2635	0.2085	0.2034	0.1416	0.9189	0.9151	95.2381	100
23	0.1701	0.2032	0.1219	0.139	0.9228	0.9152	80.9524	95.2381
24	0.1755	0.2012	0.1262	0.1374	0.9235	0.9151	80.9524	95.2381
25	0.191	0.2004	0.1382	0.1367	0.9238	0.9151	80.9524	95.2381
26	0.1139	0.1929	0.0831	0.1319	0.938	0.9155	33.3333	90.4762
27	0.1152	0.1921	0.0837	0.1315	0.9389	0.9156	33.3333	90.4762
28	0.1224	0.1894	0.09	0.1292	0.9414	0.9159	33.3333	90.4762
29	0.1297	0.1875	0.0962	0.1276	0.9429	0.9162	33.3333	90.4762
30	0.1358	0.1865	0.0993	0.1271	0.9436	0.9165	33.3333	90.4762
31	0.1536	0.1854	0.1165	0.126	0.9445	0.9163	33.3333	90.4762
32	0.1605	0.1852	0.1243	0.1258	0.9446	0.9162	38.0952	90.4762
33	0.1703	0.1853	0.1389	0.1259	0.9444	0.9162	38.0952	90.4762

When DFIG is connected adjacent to SEIG at wind speed of 12m/s, only 14% of the buses suffer from the undervoltage problem. The maximum average voltage is 0.9592 p.u. The minimum active and reactive power losses are 0.1131 p.u and 0.1796 p.u at location 6, respectively as given in Table 7. When wind speed is reduced to 8m/s, SEIG loses its excitation and acts as additional

reactive load on the network. In this case, the average voltage falls to 0.9118 p.u and power loss increases beyond the base case value. 90% of the buses suffer from the undervoltage problem. When DFIG acts as a reactive source and supplies the necessary reactive power to SEIG, the undervoltage buses reduce to 80.9% and average voltage rises to 0.9257 p.u. The active and reactive power loss reduce to 0.158 p.u and 0.1215 p.u, respectively. The results show that reactive power supplied from DFIG is capable of protecting SEIG from voltage collapse, thereby aiding the stability of the network. The comparative analysis of ability of DFIG and D-STATCOM in stabilizing SEIG is explained in detail in the following sections.

ANALYSIS OF RESULTS

The methods used for voltage control of SEIG presented in section 5 are compared and analysed in this section. This section of comparing results is divided into three categories as power loss, average voltage, and RUVMN. The comparisons of results are given in Table 8.

Table 8. Comparison of ability of D-STATCOM and DFIG to stabilize SEIG at low wind speed (8m/s).

Location	Ploss (p.u)		Qloss (p.u)		Average voltage (p.u)		% RUVMN	
	Case 1	Case 2	Case 1	Case 2	Case 1	Case 2	Case 1	Case 2
2	0.2093	0.2083	0.1423	0.1418	0.9153	0.9154	100	100
3	0.2038	0.1988	0.1394	0.1368	0.9159	0.9166	95.2381	95.2381
4	0.2005	0.1938	0.1377	0.1342	0.9164	0.9174	95.2381	90.4762
5	0.1969	0.1889	0.1358	0.1316	0.917	0.9182	90.4762	90.4762
6	0.1916	0.1783	0.1311	0.1228	0.9178	0.9198	90.4762	80.9524
7	0.1942	0.1771	0.1313	0.1193	0.9174	0.9201	90.4762	80.9524
8	0.1925	0.169	0.1301	0.1135	0.9178	0.9219	90.4762	80.9524
9	0.1921	0.1655	0.1298	0.111	0.918	0.9229	90.4762	80.9524
10	0.192	0.1626	0.1297	0.1089	0.9181	0.9238	95.2381	80.9524
11	0.1916	0.1621	0.1295	0.1087	0.9182	0.924	95.2381	80.9524
12	0.1909	0.1614	0.1291	0.1084	0.9183	0.9242	95.2381	80.9524
13	0.1915	0.1589	0.1294	0.1065	0.9183	0.9251	95.2381	80.9524
14	0.1929	0.1582	0.1302	0.1056	0.918	0.9253	95.2381	80.9524
15	0.1935	0.158	0.1306	0.1054	0.9179	0.9256	95.2381	80.9524
16	0.1938	0.158	0.1309	0.1055	0.9179	0.9257	95.2381	80.9524
17	0.1955	0.1587	0.1319	0.1063	0.9176	0.926	95.2381	80.9524
18	0.1956	0.1594	0.1321	0.1068	0.9176	0.926	95.2381	80.9524
19	0.2092	0.2083	0.1422	0.1417	0.9153	0.9154	100	100
20	0.2086	0.2078	0.1417	0.1414	0.9155	0.9158	100	100
21	0.2085	0.2079	0.1416	0.1415	0.9155	0.9159	100	100
22	0.2086	0.2084	0.1416	0.1421	0.9155	0.9159	100	100
23	0.2028	0.1968	0.1387	0.1355	0.916	0.9167	95.2381	95.2381
24	0.2014	0.1934	0.1375	0.1329	0.916	0.9169	95.2381	95.2381
25	0.2009	0.1924	0.1371	0.132	0.916	0.917	95.2381	95.2381
26	0.1903	0.1773	0.1304	0.1222	0.918	0.92	90.4762	80.9524
27	0.1887	0.176	0.1294	0.1215	0.9182	0.9202	90.4762	80.9524

28	0.1843	0.1715	0.1259	0.1177	0.9188	0.9208	80.9524	80.9524
29	0.1808	0.1684	0.1232	0.1151	0.9192	0.9213	80.9524	80.9524
30	0.1779	0.167	0.1214	0.1143	0.9196	0.9215	80.9524	80.9524
31	0.178	0.1655	0.1211	0.1129	0.9196	0.9218	80.9524	80.9524
32	0.1782	0.1654	0.1212	0.1128	0.9196	0.9218	80.9524	80.9524
33	0.1785	0.1658	0.1215	0.1134	0.9196	0.9218	80.9524	80.9524

Power loss

At wind speed of 12m/s active and reactive power loss during case 2 are less compared to case 1 and less than those of the base case in both methods. When wind speed was reduced to 8m/s and SEIG fell into unstable region, power loss in both case 1 and case 2 increases but increment is less in case 2, more than the value of the base case. During the case when SEIG is stabilized, reduction in power loss is more in case 2 compared to case 1, but both less than the value of the base case. This entire phenomenon is because of the capability of DFIG to supply active power even at low wind speeds, whereas D-STATCOM can supply only reactive power. The advances case 2 in terms of power loss compared to case 1.

Average voltage profile

At a base wind speed of 12m/s average voltage profile is within stable region in both case 1 and case 2. When wind speed falls to 8m/s driving the SEIG into underexcitation, during case 1 average voltage profile of all the locations fall drastically threatening the system stability. In case 2, the value is marginally safe because even though SEIG is acting as a reactive load, DFIG is capable of generating power at rated voltage, while a STATCOM cannot in case 1. During the compensation of SEIG reactive power requirement also the average voltage profile of the system is good in case 2 compared to case 1.

Rate of undervoltage mitigated nodes (RUVMN)

The index used in this paper explains the performance difference of case 1 and case 2 in detail. During wind speed of 12m/s only 14% of the buses are facing undervoltage problem in case 2, whereas in case 1, 28% of the buses face undervoltage problem. When wind speed reduces to 8m/s and SEIG acting as a reactive load, few of the locations face 95% of undervoltage bus problem. In case 2, major locations face 90% and only less number of locations face 100% RUVMN because DFIG is generating active power even at low wind speeds. During the scenario of SEIG generating active power in a stable region, in case 1 the majority of locations face 90% of undervoltage buses, whereas in case 2, the majority of locations face 84% of undervoltage buses. Even though some of the locations have 84% undervoltage buses, the choice of best location is limited if power loss and average voltage are also cumulatively considered. The results show that in every scenario the numbers of buses facing undervoltage are less in case 2 compared to case 1.

CONCLUSION

The results show that both D-STATCOM and DFIG are capable of handling reactive power requirements of SEIG as well as achieving network stability. During the case of low wind of speed (8m/s) both methods assist SEIG in escaping from voltage collapse, thereby enhancing network stability. But the proposed method exhibits superiority during both underexcited case and when

supplying reactive power to SEIG. This is because DFIG has the ability to supply active power even during low wind speeds and in reactive power control mode, it can supply reactive power as well. In case of D-STATCOM, it can provide only reactive power support during normal and underexcited case but not active power. The developed equivalent capacitance model of DFIG demonstrates the reactive power handling capabilities effectively. In economic terms also the proposed method is the best among the existing methods because no additional equipment is necessary to stabilize the system; DFIG already present in the system is well enough to stabilize SEIG. This developed model can also be extended for load flow analysis of multimachine system during time varying loads and fault conditions very effectively. The performance of D-STATCOM can be enhanced by using an active source like solar charged battery as input to facilitate both active and reactive power control. The active power loss, reactive power loss, average voltage, and RUVMN can be considered as objectives for optimal load flow solution.

APPENDIX

Calculation of minimum capacitance requirement of SEIG

The minimum capacitance requirement for a given wind speed is calculated by the following equations (Malik *et al.*, 1987)

$$C_{\min} = \frac{1}{2\pi}(\frac{X_l f}{M_3} + \frac{M_4}{M_1^2 + M_2^2}) \tag{22}$$

where the coefficients in Equation (22) are given by

$$M_1 = R_s R_r - f((f-v)*(x_s x_r + x_s x_m) + x_r x_m) \tag{23}$$

$$M_2 = R_r f(x_s + x_m) + R_s (f-v)(x_r + x_m) \tag{24}$$

$$M_3 = R_L^2 + X_L^2 f^2 \tag{25}$$

$$M_4 = R_r M_2 + (x_r + x_m)f(f-v)M_1 \tag{26}$$

where f, v are p.u frequency and speed.

The parameters (Dadhani et al., 2013) of the induction machine considered for the study are presented in Table A1.

Table A1. Induction machine parameters.

Wound rotor induction machine stator/grid voltage V_S (r.m.s. L-L)	2400 V
Nominal power S: 2250 hp *746 VA	1.6MVA
Nominal phase voltage V (Per Phase)	1368 V
Nominal frequency (f)	50 Hz
Stator resistance (R_s)	0.029 Ω
Stator inductance (L_{sl})	0.226/377 H

Rotor resistance (R_r)	0.022 Ω
Rotor inductance (L_{rl})	0.226/377 H
Mutual inductance (L_{ml})	13.04/377 H
Inertia coefficient (J)	63.87
Pole pairs (P)	2
Pitch angle(β)	0 degree
Data nominal mechanical output power (P_{nom})	1.5 MW
Base power of the electrical generator (S_b)	2250 hp
Base wind speed (ω_{base})	14 m/s
Max. power at base wind speed (p.u. of nominal mech. power)	0.73
Base speed (p.u. of base generator speed)	1.2
Excitation capacitance (each phase) (C)	68μF
Z_g (impedance of grid side and rotor side converter)	0.345 Ω

Table A2. Parameters of IEEE 33-bus system without DG.

Active power loss (kW)	Reactive power loss (kW)	Average voltage (P.U)	Number of undervoltage buses (bus no.)
210.2	142.95	0.9137	**21**(6,7,8,9,10,11,12, 13,14,15,16,17,18,26, 27,28,29,30,31,32,33

REFERENCES

Bansal, R. C. 2005. Three Phase Induction generators: An Overview. IEEE Trans. Energy Convers. 20(2):292-299

Mustafa A. Al-Saffar Eui-Cheol Nho, Thomas A. & Lipo, 1998. Controlled shunt capacitor self-excited induction generator. IEEE Conference on Industrial App 2:1486-1490.

Malik, N. H. & Mazi, A. A. 1987. Capacitance requirements of self-excited induction generators. IEEE Trans. on Energy Conversion 2(1): 2-9.

Kheldoun, A., Refoufi, L. & Eddine, D. 2012. Analysis of the self-excited induction generator steady state performance using a new efficient algorithm. Journal of Electr. Power Syst 86: 61–67.

Rajambal, K., Umamaheswari, B. & Chellamuthu, C. 2005. Electrical braking of large wind turbines. Renewable Energy. 30(15): 2235–2245.

Muyeen, S. M., Ali, M. H., Murata, T. & Tamura J. 2006. Transient stability enhancement of wind generator by a new logical pitch controller. IEEE Trans. Power Energy 126(8):742–752.

Muyeen, S. M., Mannan, M. A., Ali, M. H., Takahashi, R., Murata, T. & Tamura, J. 2006. Stabilization of wind turbine generator system by STATCOM. IEEJ Trans. Power Energy 126(10):1073–1082.

Saoud, Z. S., Lisboa, M. L., Ekanayake, J. B., Jenkins, N. & Strbac, G. 1998. Application of STATCOMs to wind farms Proc. IEE Gener. Transm. Distrib. 145(5):511–516.

Hosseini, M., Shayanfar, H. A. & Firuzabad, M. F. 2008. Modeling of series and shunt Distribution FACTS devices in distribution system Load flow. Journal of Electrical Systems 4: 1-12.

Mohd. H. A. & Bin W. 2010. Comparison of Stabilization Methods for Fixed-Speed Wind Generator Systems," IEEE Trans. on Power Delivery 35(1).

Muyeen, S. M., Mannan, M. A., Ali, M. H., Takahashi, R., Murata, T., Tamura, J., Tomaki, Y., Sakahara, A. & Sasano, E. 2007. Comparative study on transient stability analysis of wind turbine generator system using different drive train models. IET Renew. Power Gener. 1(2):131–141.

Divya, K. C., Rao & P. S. N. 2006. Models for wind turbine generating systems and their application in load flow studies. Electric Power Syst. Research 76: 844–856.

Ullahand N. R. & Thiringer, T. 2007. Variable Speed Wind Turbines for Power System Stability Enhancement. IEEE Trans. Energy conver. 22(1):52–60.

Kayikci, M. & Milanovic, J. V. 2007. Reactive power control strategies for DFIG based plants. IEEE Trans. Energy Convers. 22(2): 389–396.

Ekanayake, J. B., Holdsworth, L., Xue Guang Wu & Jenkins, N. 2003. Dynamic modeling of doubly-fed induction generator wind turbines. IEEE Trans. Power Syst. 18(2): 803–809.

Tapia. 2003. Modeling and control of a wind turbine driven doubly fed induction generator. IEEE Transactions on Energy Conversion 18:194-204.

Feijóo & Cidrás, J. 2010. Calculating Steady-State Operating Conditions for Doubly-Fed Induction Generator Wind Turbines. IEEE Trans. Power Syst.25(2): 922–928.

Dadhani, A., Venkatesh, B., Nassif, A. B. & Sood, V. K. 2013. Modeling of Doubly fed Induction Generators for Distribution system Power flow analysis Electric Power and Energy Systems 53: 576-583.

Takahashi, R., Tamura, J., Futami, M., Kimura, M. & lde K. 2006. A New Control Method for Wind Energy Conversion System Using Double Fed Synchronous Generator. IEEJ Power and Energy 126(2):225-235.

Chowdhury, B. H. & Chellapilia, S. 2006. Doubly-fed induction generator control for variable speed wind power generation. Electric Power System Research 76: 786-800.

Mohseni, M., Islam, S. M. & Masoum, M. A. S. 2011. Enhanced hysteresis-based current regulators in vector control of DFIG wind turbines. IEEE Trans. Power Electron. 26(1) :223-234.